Journal of Vacuum Science & Technology B

High-quality nanothick single-crystal Y 2 O 3 films epitaxially grown on Si (111): Growth and structural characteristics

Y. J. Lee, W. C. Lee, C. W. Nieh, Z. K. Yang, A. R. Kortan, M. Hong, J. Kwo, and C.-H. Hsu

Citation: Journal of Vacuum Science & Technology B **26**, 1124 (2008); doi: 10.1116/1.2889387
View online: http://dx.doi.org/10.1116/1.2889387
View Table of Contents: http://scitation.aip.org/content/avs/journal/jvstb/26/3?ver=pdfcov
Published by the AVS: Science & Technology of Materials, Interfaces, and Processing

Articles you may be interested in

Nanometer thick single crystal Y 2 O 3 films epitaxially grown on Si (111) with structures approaching perfection
Appl. Phys. Lett. **92**, 061914 (2008); 10.1063/1.2883939

High-quality nanothickness single-crystal Sc 2 O 3 film grown on Si(111)
Appl. Phys. Lett. **87**, 251902 (2005); 10.1063/1.2147711

High-quality thin single-crystal - Al 2 O 3 films grown on Si (111)
Appl. Phys. Lett. **87**, 091908 (2005); 10.1063/1.2037205

Structural and electrical quality of the high-k dielectric Y 2 O 3 on Si (001): Dependence on growth parameters
J. Appl. Phys. **92**, 426 (2002); 10.1063/1.1483379

Temperature dependence of the properties of heteroepitaxial Y 2 O 3 films grown on Si by ion assisted evaporation
J. Appl. Phys. **86**, 198 (1999); 10.1063/1.370717

Re-register for Table of Content Alerts

Create a profile.

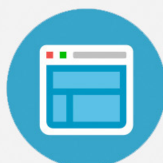

Sign up today!

Redistribution subject to AVS license or copyright; see http://scitation.aip.org/termsconditions. Download to IP: 140.113.38.11 On: Wed, 30 Apr 2014 23:06:38

High-quality nanothick single-crystal Y_2O_3 films epitaxially grown on Si (111): Growth and structural characteristics

Y. J. Lee, W. C. Lee, C. W. Nieh, Z. K. Yang, A. R. Kortan, and M. Hong[a)]
Department of Materials Science and Engineering, National Tsing Hua University, Hsinchu, Taiwan 30013, Republic of China

J. Kwo[b),c)]
Department of Physics, National Tsing Hua University, Hsinchu, Taiwan 30013, Republic of China

C.-H. Hsu[b),d)]
National Synchrotron Radiation Research Center, Hsinchu, Taiwan 30076, Republic of China

(Received 26 October 2007; accepted 4 February 2008; published 30 May 2008)

High-quality single-crystal nanothick Y_2O_3 films have been grown epitaxially on Si (111) despite a lattice mismatch of 2.4%. The films were electron beam evaporated from pure compacted powder Y_2O_3 target in ultrahigh vacuum. Y_2O_3 3 nm thick exhibited a bright, sharp, streaky reconstructed (4×4) reflection high energy electron diffraction pattern. Structural studies carried out by x-ray diffraction with synchrotron radiation and high-resolution transmission electron microscopy show that the films have the cubic bixbyite phase with a remarkably uniform thickness and high structural perfection. Two Y_2O_3 domains of *B*-type Y_2O_3 $[2\bar{1}\bar{1}]\|\mathrm{Si}[11\bar{2}]$ and *A*-type Y_2O_3 $[2\bar{1}\bar{1}]\|\mathrm{Si}[2\bar{1}\bar{1}]$ coexist in the initial film growth with *B* type predominating over *A* type in thicker films as studied using x-ray diffraction. The narrow full width at half maximum of 0.014° in the ω-rocking curve is the characteristic of excellent crystalline films. High-resolution transmission electron microscopy and fast Fourier transform analysis show atomically sharp interface and strain relaxation in thicker films. © *2008 American Vacuum Society.* [DOI: 10.1116/1.2889387]

I. INTRODUCTION

Heteroepitaxial growth of insulators on semiconductors has always been of great interest in science and of importance in technology. For example, epitaxial growth of insulators on Si may find applications in fabrication of silicon-on-insulator and three-dimensional Si integrated circuits. Additional application is found in the efforts of high *k* dielectrics on Si (Refs. 1 and 2) and other semiconductors with high carrier mobility,[3,4] a very urgent technological issue. A subsequent single-crystalline growth of other semiconductors such as GaN (Ref. 5) on these single-crystal insulators may integrate high-power microwave devices or lasers with the most advanced Si-based electronic devices.

Many attempts have been taken to grow epitaxial Y_2O_3 films on Si,[1,6–8] due to a small lattice mismatch of −2.4% between Si $[2\times a(\mathrm{Si})=1.086$ nm$]$ and cubic phase Y_2O_3 $[(a(Y_2O_3)=1.060$ nm$]$. Y_2O_3 (110) was found to epitaxially grow on Si (100) with two degenerate domains of an equal population.[1,7] The degeneracy was removed with the employment of vicinal (001) Si substrates of 4° miscut along $[1\bar{1}0]$, resulting in the growth of mostly single-domain (110) orientated epitaxial films.[1,7] For growing Y_2O_3 on Si (111),[8] it has been difficult to achieve a good epitaxial Y_2O_3 (111) layer of a few nanometers thick on Si (111). For example, epitaxial Y_2O_3 films on Si (111) were prepared by the reaction of evaporated yttrium under an oxygen partial pressure (10^{-6} torr) for a film thickness of ~75 nm.[8] An oxidized Si surface [4° vicinal (111) orientation] with a SiO_2 layer 1.5 nm thick was needed to achieve better quality epitaxy while islandlike growth was found on a clean Si surface.

In this paper, an excellent growth of nanothick Y_2O_3 (111) has been achieved on Si (111) with an atomically smooth interface and a record-small full width at half maximum (FWHM) ~0.014° in rocking scans obtained in films of thickness less than 10 nm. The oxide films were deposited from electron-beam evaporation of a powder-packed Y_2O_3 target in ultrahigh vacuum (UHV). X-ray scattering and reflectivity using a synchrotron radiation source, and a high-resolution transmission electron microscopy (HRTEM) were used to study the Y_2O_3/Si (111) heteroepitaxial system for the dielectric layers from 2 to 10 nm in thickness.

II. EXPERIMENT

Si (111) wafers were cleaned by the Radio Corporation of America method, and hydrogen passivated by a buffered hydrofluoric acid solution, before being put into a multichamber molecular beam epitaxy/electron-beam evaporation UHV system.[9] After being heated to 700 °C, the Si surface exhibited a conversion from a weak (1×1) to a bright (7×7) reconstructed reflection high energy electron diffraction (RHEED) pattern with Kikuchi arcs [Fig. 1(a)], indicating a clean Si surface free of contaminations or native oxides.[10] A thin Y_2O_3 film was then deposited on the reconstructed Si surface, with substrate temperature maintained at about

a)Electronic mail: mhong@mx.nthu.edu.tw
b)Authors to whom correspondence should be addressed
c)Electronic mail: raynien@phys.nthu.edu.tw
d)Also at Department of Photonics, National Chiao Tung University, Hsinchu, Taiwan 30010, Republic of China; electronic mail: chsu@nsrrc.org.tw

Redistribution subject to AVS license or copyright; see http://scitation.aip.org/termsconditions. Download to IP: 140.113.38.11 On: Wed, 30 Apr 2014 23:06:38

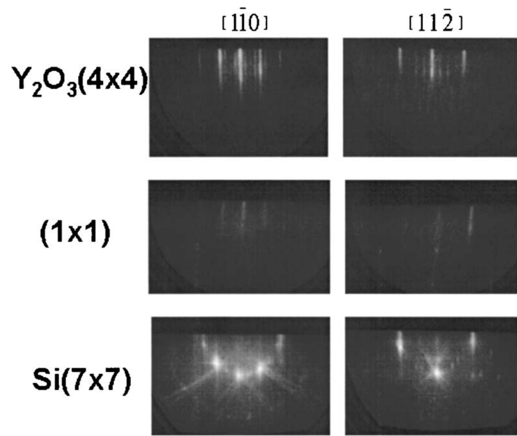

FIG. 1. *In situ* RHEED patterns of Si (111) substrate and ~3 nm thick Y_2O_3 films along the [1$\bar{1}$0] and [11$\bar{2}$] axes.

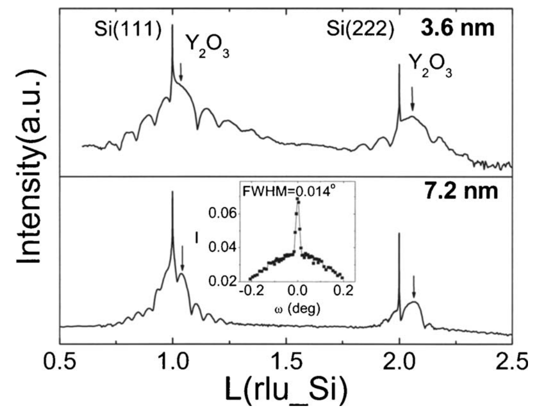

FIG. 2. Radial scans along the Si (111) substrate normal of two samples with 3.6 and 7.2 nm thick Y_2O_3 layers, where the arrows mark the Bragg reflections of Y_2O_3. The inset shows the ω-rocking curve of the 7.2 nm thick Y_2O_3 film.

780 °C. A (1×1) oxide RHEED pattern [Fig. 1(b)] appeared right after the oxide deposition along with the reconstructed (7×7) of weaker intensity from the Si beneath, which disappeared after the oxide growth up to 0.3–0.4 nm. The (1×1) oxide RHEED pattern persisted until the appearance of a reconstructed (4×4) streaky RHEED pattern. The sharp bright (4×4) pattern, as shown in Fig. 1(c), was observed after the growth of the Y_2O_3 film ~3 nm thick, indicating attainment of a high-quality crystalline film with an atomically smooth surface. After deposition, the sample was capped with a thin layer of Si for protection, as the rare-earth oxide tends to absorb moisture with air exposure.[11]

HRTEM specimens were prepared with mechanical polishing, dimpling, and ion milling using a Gatan PIPS system operated at 4 kV. HRTEM images were taken using a field-emission microscopy (JEM-2100F) operated at 200 kV. For better understanding of the obtained TEM pictures, we have carried out a fast Fourier transform (FFT) analysis on digitally saved TEM images.

The synchrotron x-ray measurements were performed at wiggler beamline BL17B1 at the National Synchrotron Radiation Research Center, Hsinchu, Taiwan, and the detailed experimental procedure was described in Ref. 12. High-resolution x-ray measurements were carried out in single-crystal geometry. X-ray reflectivity measurements were performed to determine film thickness and surface/interfacial roughness.[13,14] A hexagonal unit cell (h) was adapted by coordinate transformation from commonly used cubic unit cell to decouple the normal and in-plane components of momentum transfer in x-ray scattering measurements. In reciprocal space, the basis vectors are transformed in the following: $(100)_h=(4\bar{2}\bar{2})/3$, $(010)_h=(22\bar{4})/3$, and $(001)_h=(111)/3$, where the momentum transfer in the direction normal to the interface is represented by a single index l.[12]

III. RESULTS AND DISCUSSION

X-ray diffraction (XRD) was used to analyze the phase and crystallographic orientation of Y_2O_3 layers deposited on Si (111). Figure 2 shows the radial scans along the Si $(006)_h$ crystal truncation rod (CTR) of two samples with different oxide thickness (3.6 and 7.2 nm), where the x axis is in the units of reciprocal lattice (rlu) of silicon in the hexagonal frame. The intense sharp peaks centered at 3 and 6 rlu are the Si $(003)_h$ and $(006)_h$, i.e., (222) and (444) reflections, respectively. The two strong broad peaks, centered at ~3.11 and ~6.15 rlu, are attributed to the $(006)_h$ and $(0012)_h$, i.e., (222) and (444) of Y_2O_3. Their corresponding interplanar spacing is close to d_{222} and d_{444} of cubic phase of Y_2O_3. Only the Y_2O_3 $(00l)_h$ reflections with l equal to 6 and 12 were observed on the radial scans along the surface normal, indicating that the oxide films are (111) oriented with a bixbyite structure. The presence of periodic Pendellosung fringes which originate from the interference between the top and buried interfaces reveals the atomically smooth interfaces and the high crystalline quality of the deposited layer. Estimated from the FWHM of Y_2O_3 $(0012)_h$ reflections for different oxide thickness, the coherence length along the growth direction is always comparable to the film thickness, implying that the structural coherence extends over the whole film thickness.

To further examine the crystalline quality of the oxide films, we also performed ω-rocking scan on the samples. A very narrow peak with a FWHM of 0.017° for a 3.6 nm thick film [slightly wider than the 0.008° FWHM of the nearby Si $(006)_h$ reflection] was measured; an even smaller peak width ~0.014° (as shown in the insert of Fig. 2) was obtained for thicker films. Such narrow rocking curves reveal the small mosaicity and highly perfect crystalline structure of the grown films. With increasing layer thickness, e.g., 7.2 nm, the film structure gradually relaxes through the generation of dislocation, leading to the appearance of an additional broad component in the rocking curve. With thickness further increasing to 9.5 nm, misfit dislocations and their induced strain fields would be gradually buried below and the broad component of the rocking curves gradually becomes narrower.

The strain state of the films was determined from the lattice spacing along normal and lateral directions (not shown).

Redistribution subject to AVS license or copyright; see http://scitation.aip.org/termsconditions. Download to IP: 140.113.38.11 On: Wed, 30 Apr 2014 23:06:38

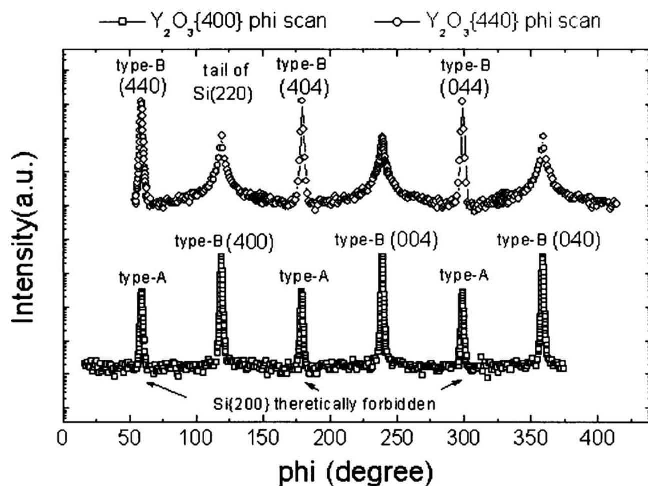

FIG. 3. Phi cone scan of 9.5 nm thick Y_2O_3 over the family of cubic Y_2O_3 {400} and {440} reflections confirming a threefold symmetry and the coexistence of A/B type (111) domains.

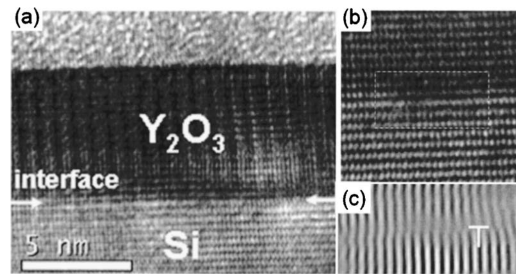

FIG. 4. (a) Cross-sectional HRTEM image of a 7.2 nm thick epitaxial Y_2O_3 film grown on Si (111) substrate along the Si $[11\bar{2}]$ projection. (b) Enlarged magnification of the interface between Y_2O_3 film and Si substrate. (c) Fourier filtered image of (b) using spatial frequency. Misfit dislocations were observed at the interface with "T" mark.

Over the range of film thickness investigated, a monotonic decrease/increase of normal/lateral lattice spacing was observed. For the thinnest film studied, 1.6 nm thick, the measured in-plane strain is ~1.5%, significantly less than the 2.5% expected for a fully strained layer. Up to 9.5 nm thick, the lattice of Y_2O_3 films is not fully relaxed, and a lateral strain ~0.4% still remains. X-ray scattering results indicate that for Y_2O_3 films of thickness less than 10 nm, the lattice changes from a highly strained stage to a nearly fully relaxed one with increasing film thickness.

Azimuthal scans (ϕ scan) across Y_2O_3 $\{028\}_h$ and $\{204\}_h$, i.e., {440} and {400}, respectively, were performed to examine the relative in-plane orientation and the ratio between two types of rotational domains. The phi scans of a 9.5 nm thick Y_2O_3 film are shown in Fig. 3 as an example. The broad peaks that appeared in the Y_2O_3 {440} phi scan came from the tail of Si {220} CTRs; the 60° offset between these two sets of peaks reveals that the $[1\bar{1}0]$ in-plane axis of the Y_2O_3 film is rotated 60° from that of the Si substrate, known as the B-type (111) oriented domain with Y_2O_3 $[2\bar{1}\bar{1}] \parallel$ Si $[11\bar{2}]$. Furthermore, two sets of sharp peaks with nearly equal peak width were observed in the Y_2O_3 {400} ϕ scan. The stronger set is the B-type domain, having the same origin as the sharp peaks in the {440} ϕ scan. Because nearby Si {200} peaks are forbidden reflections and extremely weak, we can ensure that the set of weaker peaks originates from a second Y_2O_3 domain with its in-plane axes aligned with those of the Si substrate, the A-type domain with Y_2O_3 $[2\bar{1}\bar{1}] \parallel$ Si $[2\bar{1}\bar{1}]$. The ratio between the dominant B-type domain and the minor A-type domain grows with film thickness, with the fraction of B-type domain exceeding 90% as the film thickness >5 nm.

A representative cross-sectional HRTEM image of the crystalline Y_2O_3 film 7.2 nm thick along the Si $[11\bar{2}]$ projection is shown in Fig. 4(a). It reveals a sharp Y_2O_3/Si interface, which was magnified and displayed in Fig. 4(b). To analyze the interfacial structure in more detail, a masking step and an inverse fast Fourier transform (IFFT) were applied to the FFT results. That is, a specific diffraction pattern in reciprocal space was chosen by the spot-shaped mask pattern and then IFFT was performed. Figure 4(c) shows the Fourier filtered image of the area enclosed by a rectangle in Fig. 4(b). Misfit dislocations were marked "T" at the interface. The location of an edge component of misfit dislocation is clearly shown at the interface. These linear defects provide a relaxation mechanism for the strained lattice. It is well known that the presence of misfit dislocations is a characteristic structural feature of epitaxial thin films grown on dissimilar substrates with a large lattice mismatch. With a lattice mismatch of 2.4% between Y_2O_3 and Si, the 7.2 nm oxide thickness exceeds the critical thickness and consequently strain has been partially relaxed. This result is consistent with the lattice relaxation observed in the XRD measurements.

IV. CONCLUSIONS

Excellent crystalline quality of nanothick single-crystal Y_2O_3 films on Si (111) has been achieved. The oxide/Si heterostructure has atomically smooth interfaces, as studied using high-resolution x-ray diffraction with synchrotron radiation and high-resolution transmission electron microscopy. Two rotational domains coexist in the Y_2O_3 films, with the population of the predominant B-type domain increasing with thickness.

ACKNOWLEDGMENTS

The authors wish to thank the National Science Council of Taiwan for supporting this work, and the Center for Nano Science and Technology at NCTU, Taiwan for the help in TEM.

[1]J. Kwo *et al.*, Appl. Phys. Lett. **77**, 130 (2000).
[2]R. A. Mckee, F. J. Walker, and M. F. Chrisholm, Phys. Rev. Lett. **81**, 3014 (1998).
[3]M. Hong, J. Kwo, A. R. Kortan, J. P. Mannaerts, and A. M. Sergent, Science **283**, 1897 (1999).
[4]M. Hong, J. Kwo, P. J. Tsai, Y. C. Chang, M. L. Huang, C. P. Chen, and T. D. Lin, Jpn. J. Appl. Phys., Part 1 **46**, 3167 (2007).
[5]M. Hong *et al.*, J. Vac. Sci. Technol. B **20**, 1274 (2002).

Redistribution subject to AVS license or copyright; see http://scitation.aip.org/termsconditions. Download to IP: 140.113.38.11 On: Wed, 30 Apr 2014 23:06:38

[6]S. Guha, E. Cartier, M. A. Gribelyuk, N. A. Bojarczuk, and M. C. Copel, Appl. Phys. Lett. **77**, 2710 (2000) and the references therein.
[7]J. Kwo *et al.*, J. Appl. Phys. **89**, 3920 (2001).
[8]M. H. Cho, D. H. Ko, Y. K. Choi, I. W. Lyo, K. Jeong, and C. N. Whang, Thin Solid Films **402**, 38 (2002) and references therein.
[9]M. Hong, J. P. Mannaerts, J. E. Bowers, J. Kwo, M. Passlack, W.-Y. Hwang, and L. W. Tu, J. Cryst. Growth **175/176**, 422 (1997).
[10]M. Hong *et al.*, Appl. Phys. Lett. **87**, 251902 (2005).
[11]M. Hong, Z. H. Lu, J. Kwo, A. R. Kortan, J. P. Mannaerts, J. J. Krajewski, K. C. Hsieh, L. J. Chou, and K. Y. Cheng, Appl. Phys. Lett. **76**, 312 (2000).
[12]C. H. Hsu, P. Chang, W. C. Lee, Z. K. Yang, Y. J. Lee, M. Hong, J. Kwo, C. M. Huang, and H. Y. Lee, Appl. Phys. Lett. **89**, 122907 (2006).
[13]Y. L. Huang, P. Chang, Z. K. Yang, Y. J. Lee, H. Y. Lee, H. J. Liu, J. Kwo, J. P. Mannaerts, and M. Hong, Appl. Phys. Lett. **86**, 191905 (2005).
[14]D. Y. Noh, Y. Hwu, H. K. Kim, and M. Hong, Phys. Rev. B **51**, 4441 (1995).

Redistribution subject to AVS license or copyright; see http://scitation.aip.org/termsconditions. Download to IP: 140.113.38.11 On: Wed, 30 Apr 2014 23:06:38